DD

Invited talk at the International Symposium on Strangeness Quark Matter, Sept. 1-5, 1994, Krete, Greece. Published in the Conference Proceedings.

Preprint Bern BUHE-95-1

SEARCH FOR STRANGE QUARK MATTER IN RELATIVISTIC HEAVY ION COLLISIONS AT CERN (NA52)

KLAUS PRETZL
Laboratory for High Energy Physics, University of Bern, Sidlerstr. 5, Bern, Switzerland, 3012

and

J. BERINGER, K. BORER, F. DITTUS, D. FREI, E. HUGENTOBLER, R. KLINGENBERG, U. MOSER, T. PAL, J. SCHACHER, F. STOFFEL, W. VOLKEN
Laboratory for High Energy Physics, University of Bern, Sidlerstr. 5, Bern, Switzerland, 3012

K. ELSENER, K.D. LOHMANN
CERN, PPE-Div., Geneva 23, Switzerland, 1211

C. BAGLIN, A. BUSSIERE, J.P. GUILLAUD
IN2P3, LAPP Annecy, BP 110, Ch. du Bellevue, Annecy-le-Vieux CEDEX, France, 74941

T. LINDEN, J. TUOMINIEMI
Dept. of Physics, University of Helsinki, P.O. Box 9, Helsinki, Finland, 00014

G. APPELQUIST, C. BOHM, B, SELLDEN. Q.P.ZHANG
Dept. of Physics, University of Sweden, Box 6730, Stockholm, Sweden, 11385

PH. GORODETZKY
CRN, Centre de Recherches Nucléaires Strasbourg CEDEX, France, 67037

ABSTRACT

The NA52 experiment will search for long-lived massive strange matter particles, so-called strangelets, in Pb-Pb collisions at CERN. It will investigate the production of massive objects with a low charge to mass ratio close to zero degree production

1. Introduction

The motivation to search for strange quark matter, sometimes called "strangelets", in ultrarelativistic heavy ion collisions is twofold. First, if strange matter were to be found, it would confirm the existence of an, as yet unseen, ground state of matter; and second, it would indicate the existence of a quark gluon plasma, which on cooling [1,2] had served as a source of the strange matter.

In contrast to nuclear matter, strange quark matter consists of approximately the same number of u-, d-, and s-quarks. On the basis of the Pauli exclusion principle such multiquark states become stable owing to the introduction of strangeness as an additional degree of freedom. Strangelets can exist in neutral or charged form. By virtue of the large s-quark content, the charge to mass ratio of strangelets is expected to be small ($Z/A < 0.1$), which will be used as a promising experimental signature.

The existence of strange quark matter is not only of interest to nuclear and particle physics, but also to astrophysics. It was pointed out by E. Witten [3] that strange quark nuggets could have been produced in a first order phase transition in the early universe and could be candidates for dark matter. Also neutron stars could consist of strange quark matter [4]. It was also conjectured [5] that the "Centauro" events observed in a cosmic ray experiment could be due to an interaction between cosmic strangelets and atmospheric nuclei.

Experimental searches for strange quark matter were carried out in heavy ion collisions at the Alternating Gradient Synchrotron in Brookhaven (experiments E814, E858, E878, E886). A summary of their results can be found in Ref.[6]. Strange quark nuggets were also searched for in cosmic ray experiments [7].

In the following a description of the NA52 experiment at CERN is given and its goals are outlined.

2. Experimental Method

The experimental set up is shown in Fig.1. The secondary H6 beam line in the North Area of the SPS at CERN is used as a spectrometer. This beam line consists of a first section with a momentum focus, and a second section with an achromatic final focus. The mass of the particles produced at zero degrees in a 4cm long Pb target, will be determined from the measurements of their rigidity in the spectrometer, of their velocity with time of flight (TOF) detectors and of their charge by their energy loss (dE/dx) in the TOF counters. In the relativistic limit, the mass of the particle in terms of the measured variables is

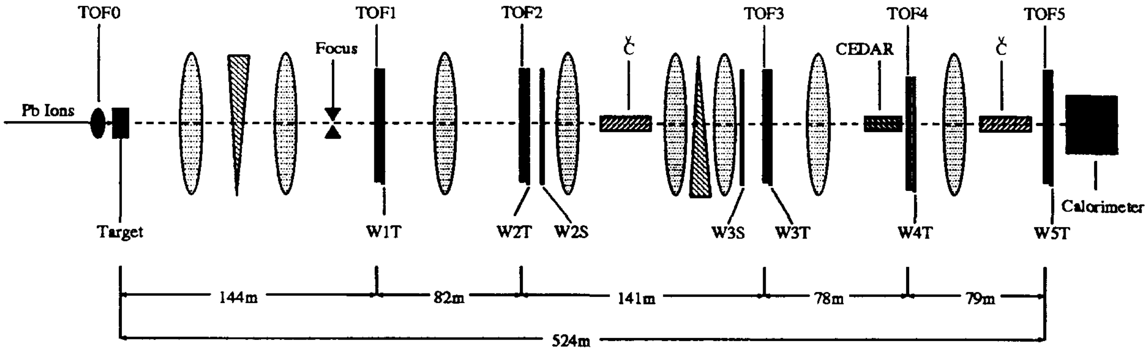

Fig.1 NA52 Experimental set up.

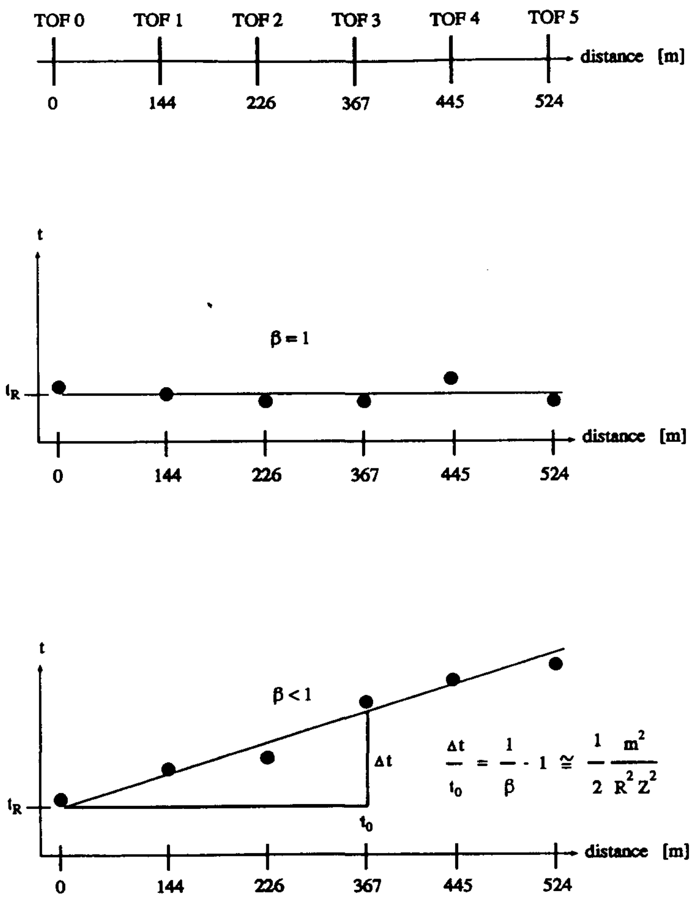

Fig.2 Velocity measurement of particles in the H6 beam spectrometer.

$$m=\sqrt{\frac{2\Delta t}{t_0}}R\cdot Z \qquad (1)$$

where $t_0 = d/c$ is the TOF of almost speed of light particles ($\beta \sim 1$) over the distance d, Δt is the measurement of the time delay of slow particles ($\beta < 1$) with respect to t_0, R is the rigidity of the spectrometer and Z the charge of the particle. The quantity $\Delta t / t_0$ is obtained from a linear fit to the arrival time measurement at the TOF counter positions along the spectrometer (Fig.2). The TOF measurement can be performed over the full length of the beam spectrometer of 524 m, requiring a particle life time $\gamma\tau > 1.8\mu s$.

Two threshold Čerenkov counters Č are used to veto light particles and to keep the trigger rate to an acceptable level of about 1500 events/spill corresponding to a dead time less than 3%. The experiment allows to choose between two types of triggers. Trigger A requires a hit in one of the TOF2 counters, a signal in an additional beam counter and no light in the first threshold Cerenkov counter. This trigger in the upstream part of the beam spectrometer allows to trigger on short lived particles which decay before reaching the downstream end of the spectrometer. Trigger A + B requires: a trigger A in the upstream part as well as a trigger B in the downstream end of the beam spectrometer. Trigger B is derived from a hit in one of the TOF4 counters, a signal in an additional beam counter and no light in the second threshold Cerenkov counter. Trigger A + B selects particles which live long enough to travel through the full length of the spectrometer. Accordingly, the data acquisition is divided into two separate sections A and B. The two independent data acquisition processors (MVME 167/OS9 System) A and B which are physically separated from each other by several hundred meters are synchronized to properly assign events in sections A and B.

Seven proportional wire chambers (W1T, W2S, W2T, W3S, W3T, W4T and W5T) are used to provide tracking for secondary particles. Each chamber is equipped with x, y and u planes. The wire spacing is 3 mm. The standard size of the chambers is 110 x 110 mm^2 covering the full beam aperture. The beam spectrometer with the proportional chambers yields a momentum resolution of $\Delta p/p < 0.85 \cdot 10^{-3}$ for particles with $p > 50$ GeV/c.

A hadron calorimeter is used at the downstream end of the spectrometer for energy measurement. This additional information provides some redundancy in the mass determination of the particle. The mass of the particle can be derived from the measured quantities

$$m = E\sqrt{1-\beta^2} \tag{2}$$

where, E is the energy of the particle and β is determined from the TOF measurement. In addition, the energy measurement for a given spectrometer rigidity provides information on the charge of the particle independent of the dE/dx measurement.

3. Target box

The so-called "target box" contains the incident ion beam counter, a remote controlled target ladder with thin target heads and 4 multiplicity counters. The target ladder and the multiplicity counters are only foreseen for a particle production experiment [8], not described here. The production target (4cm Pb) for the strangelet experiment is approximately 1m downstream of the target box.

The incident beam counter (a 400μm thick quartz disc with a diameter of 12mm) is subdivided into four optically separated sectors. The light of each sector is collected via quartz fibers onto the cathode of a XP2020 photomultiplier. The transmission of the four photomultiplier signals from the target box to the 320m distant electronics hut is done via single mode optical fibers using a Laser beam and 4 channel Mach-Zehnder modulators (Lithium Niobate) which are driven by the four photomultiplier signals. The incident beam counter is capable of handling more than 10^8 incident ions in a 5 sec spill. The signals from the incident beam counter will also be used for the time of flight measurements. They represent the TOF0 signal.

4. Time of flight counters

Five scintillation counter hodoscopes (TOF1, TOF2, TOF3, TOF4, TOF5) positioned along the beam spectrometer provide the TOF information of the particles. All five hodoscopes have the same overall dimensions, as shown in Fig.3, and cover a maximum beam aperture of $10 \times 10\,cm^2$.The width of the 8 scintillator elements (BICRON 404) varies from 8mm at the center to 20mm at the outside in order to obtain approximately the same rate in each element. The light of each hodoscope element is collected via plastic light guides onto a 2" diameter

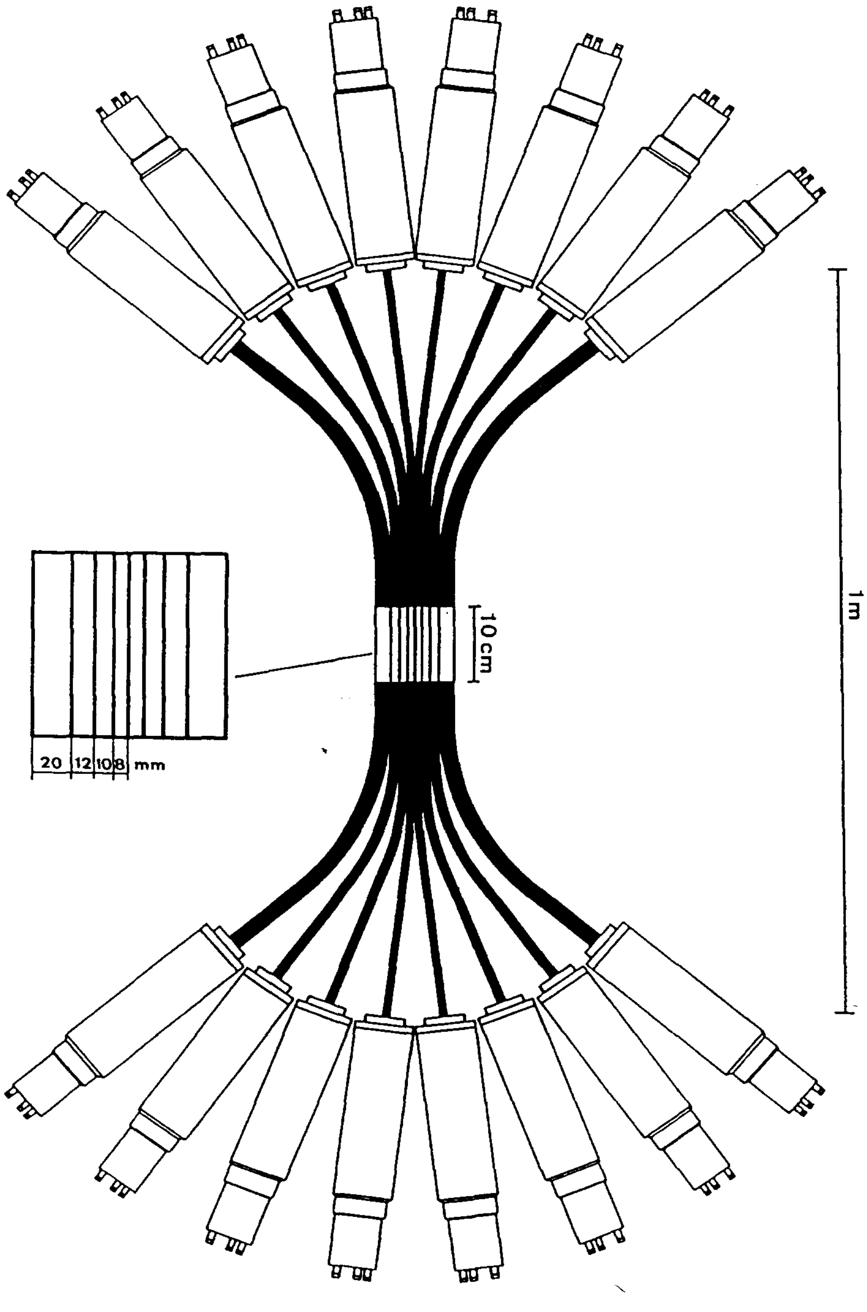

Fig.3 Time of flight (TOF) scintillation counter hodoscope.

photomultiplier (HAMAMATSU R1828-1) at each end.

The intrinsic time resolution for minimum ionizing particles (m.i.p) of TOF counter hodoscopes equipped with 1cm thick and 0.5cm thick scintillator elements were measured in a test beam. Custom made constant fraction discriminators were used. With a constant fraction of 20% a typical intrinsic time resolution of 74 ± 1ps (Fig.4) for the 1cm thick and 100 ± 1ps for the 0.5cm thick TOF counters was obtained. In order to keep the amount of material in the spectrometer as small as possible only the TOF counters which are essential for obtaining a good TOF resolution (TOF1, TOF3 and TOF5) are equipped with 1cm thick and the others (TOF2 and TOF4) with 0.5cm thick scintillators.

Fig.5 shows the time versus pulse height dependence of a TOF counter as measured with a 20% constant fraction discriminator. The flat distribution demonstrates that the use of constant fraction discriminators effectively reduces time slewing effects.

5. Hadron Calorimeter

The hadron calorimeter consists of four identical 1.5 λ_{int} deep modules of lateral dimensions 60cm x 60cm plus a fifth, back-up calorimeter module, with a depth of 1.1 λ_{int} and the same lateral dimensions. The calorimeter which was originally built by the ZEUS group [9] was recently modified for the purpose of this experiment. The first four modules each contain 45 scintillator planes, 3mm thick, interleaved with depleted uranium absorber plates of 3.2mm thickness. The fifth module contains 30 layers of 3.2mm thick uranium plates and 5mm thick scintillators. Each calorimeter module is horizontally segmented into 4 rows. The light of each row of scintillator strips is collected on the left and right sides by wavelength shifting PMMA plates, which are coupled to photomultipliers (56AVP) via light guides.

Fig.6 shows the energy resolution for electrons and hadrons measured in the H6 beam line. The comparison with the results obtained in Ref.[9] shows that the calorimeter has maintained its original performance over many years, as well as after the modification of the light collection system for this experiment.

6. Mass resolution

The mass resolution of strangelets can be estimated from the accuracy of the TOF measurement, which is assumed to be $\sigma_t/t \simeq 7.7 \cdot 10^{-5}$ (excluding TOF0) and $\sigma_t/t \simeq 5.3 \cdot 10^{-5}$ (including TOF0), and the momentum resolution of the

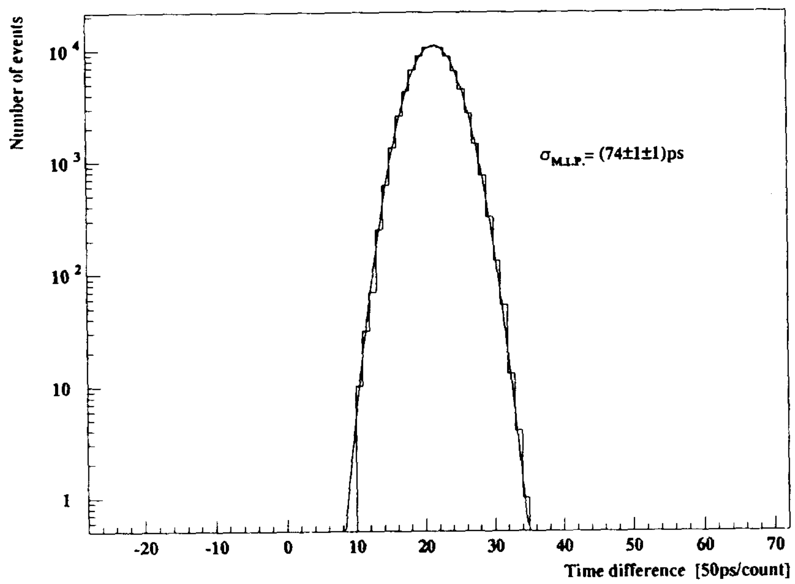

Fig.4 Intrinsic time resolution of a TOF counter with 1cm thick scintillator.

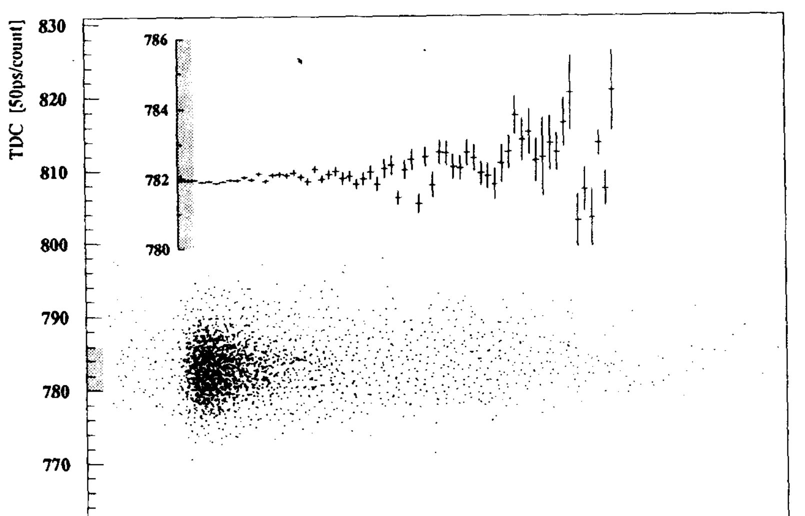

Fig.5 Time versus pulse height dependence of a TOF counter as measured with a 20%constant fraction discriminator.The minimum ionizing particles peak at around 50 ADC counts.

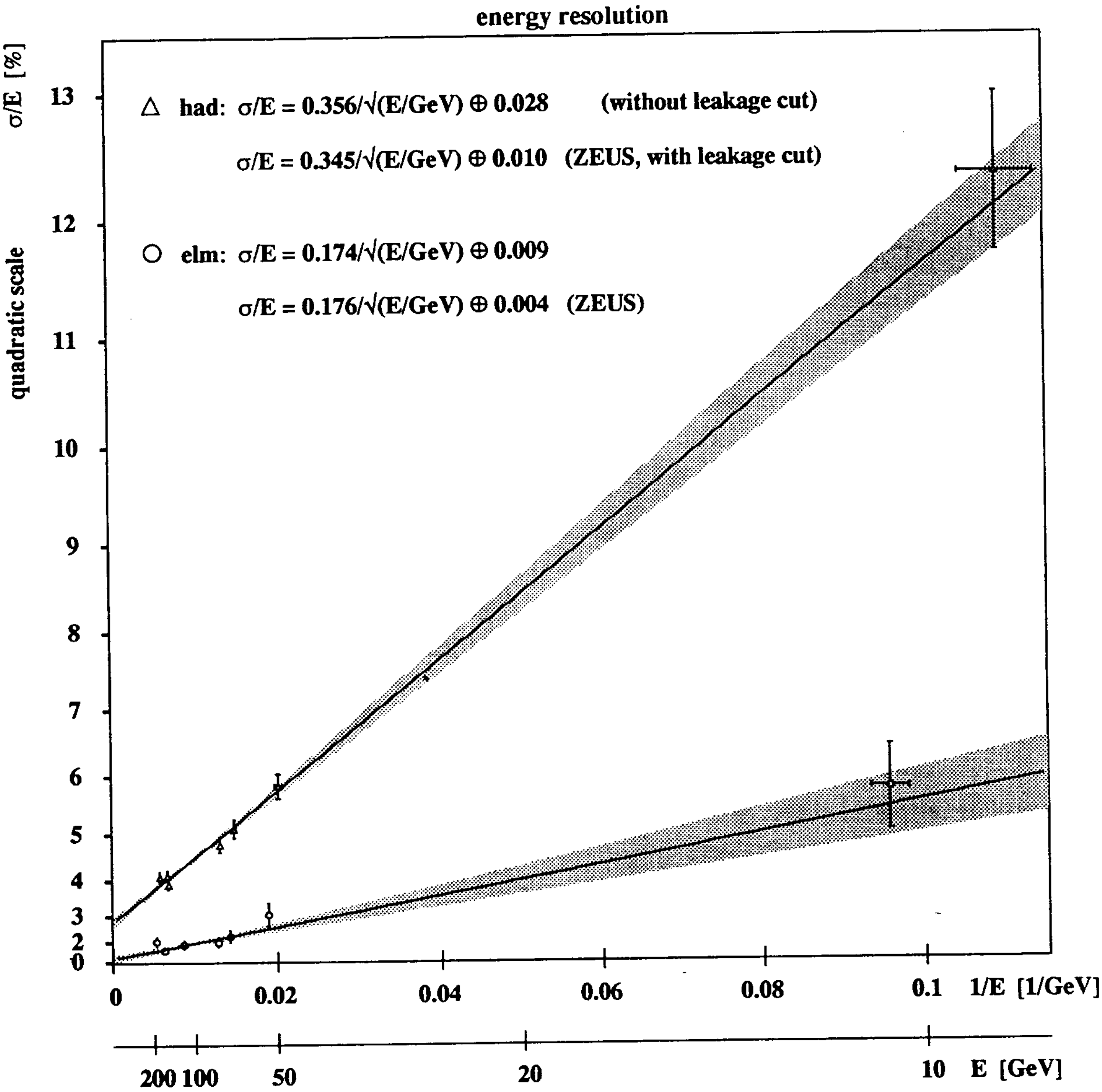

Fig.6 Energy resolution for electrons and hadrons measured with the Uranium/Scintillator hadron calorimeter.

beam spectrometer of $\sigma_p/p = 0.85 \cdot 10^{-3}$ for momenta above 50 GeV/c, using the information of the wire proportional chambers. The mass resolution can be calculated from the relation

$$\sigma_m = \sqrt{\left(m\frac{\sigma_p}{p}\right)^2 + \left(\frac{\sigma_t}{t}\,\frac{E^2}{m}\right)^2} \qquad (3)$$

and is shown in Fig.7 for strangelets with a charge Z=1 for various beam spectrometer rigidities. Multiple scattering effects are taken into account in the calculations. It can be seen that the strangelet mass resolution is dominated by the TOF measurement at low masses and by the momentum measurement at high masses.

7. Spectrometer acceptance

In order to calculate the strangelet acceptance of the beam spectrometer, a strangelet production model with a factorized phase space distribution [10] was used:

$$\frac{d^2N}{dy\,dp_t} = \frac{4p_t}{<p_t>^2}\exp\left(-\frac{2p_t}{<p_t>}\right)\frac{1}{\sqrt{2\pi}\,\sigma_y}\exp\left(-\frac{(y-\bar{y})^2}{2\sigma_y^{\,2}}\right) \qquad (4)$$

where, y is the rapidity of the strangelet, $\bar{y}$ is the rapidity of the c.m.s. of the nucleons participating in the interaction, and σ_y is the width of the rapidity distribution which was assumed to be $\sigma_y = 0.5$.

The mean transverse momentum of the strangelets is not known. In the following it is assumed that the mean transverse momentum scales with $<p_t> = a \cdot \sqrt{m}$, where m is the mass of the strangelet in GeV/c^2, and a is an arbitary parameter which can have values between 0 and 1. The $<p_t>$ of Λ's produced in oxygen gold collisions at 200 GeV/c is about 0.8 GeV/c [11] and the one of protons about 0.5 GeV/c. There is the tendency for $<p_t>$ of particles to increase as the mass increases. The parameter a depends on the production process and if strangelets are produced from a QGP via the destillation process [2] it seems reasonable to assume a rather small value for the parameter a. After the transformation $(y, p_t) \rightarrow (p, \theta)$ the fraction α of accepted strangelets can be

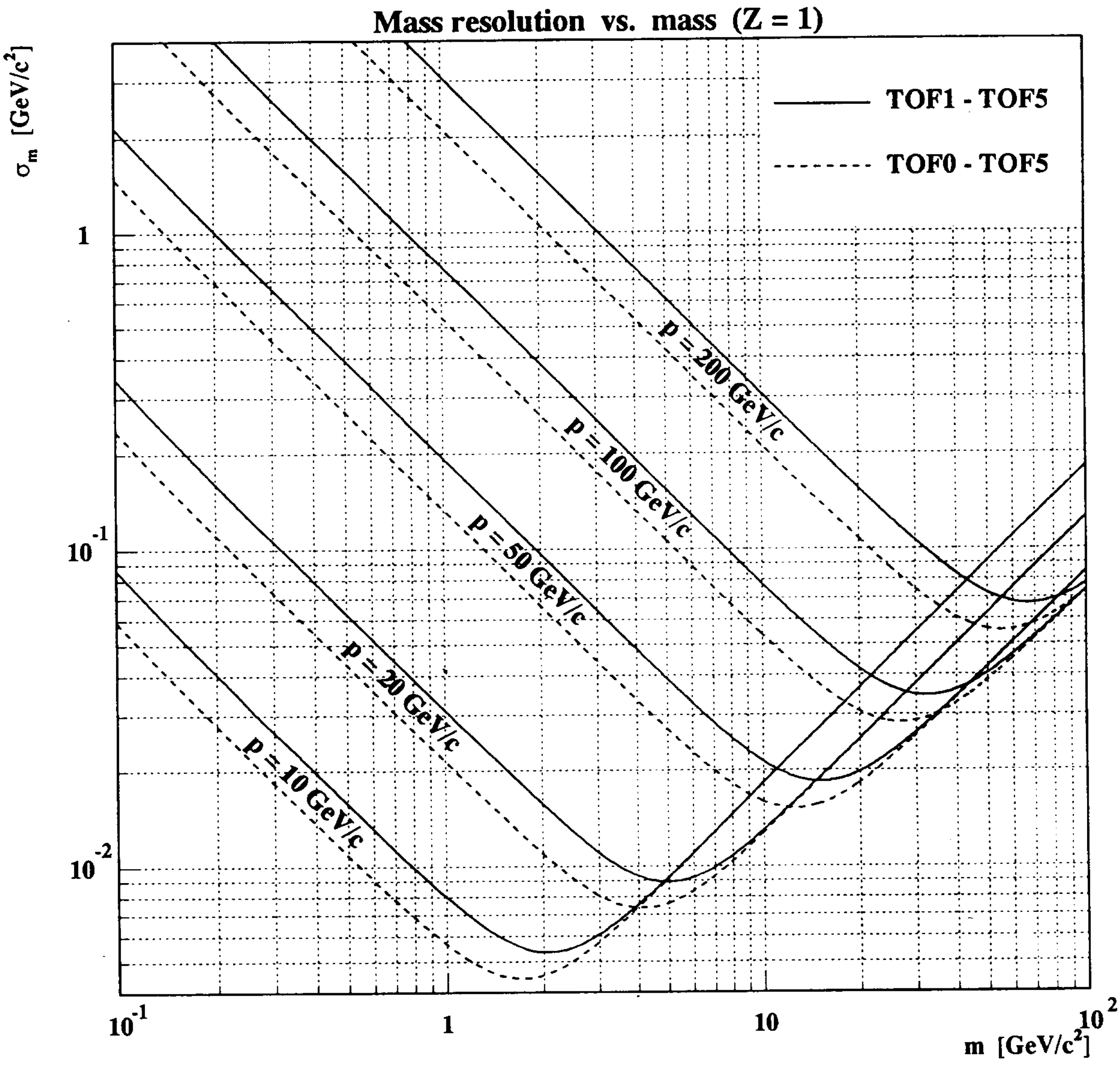

Fig.7 The mass resolution σ_m as a function of the strangelet mass, m, for different spectrometer rigidities are shown.

calculated by integrating $dN^2/dpd\theta$ over the momentum acceptance ($\Delta p/p = 3\%$) and the angular acceptance ($0 \le \theta \le 1.1$ mrad) of the H6 beam spectrometer at 0° production angle. The results are shown in Fig.8 where the ratio α/Z versus m/Z is plotted for three different spectrometer rigidities assuming $<p_t> = 0.1\sqrt{m}$ GeV/c. It should be emphasized that the results depend strongly on the model parameters. For example, with $<p_t> = 0.5\sqrt{m}$ GeV/c the acceptance α comes out to be 16 times smaller.

8. Sensitivity for strangelets

The sensitivity, S, for strangelets is defined as

$$S = \frac{1}{N_{int} \cdot \alpha \cdot \varepsilon} \qquad (5)$$

where N_{int} is the number of interactions, α is the acceptance of the beam spectrometer, as defined in the previous chapter, and ε the overall detection efficiency.

Assuming an incident beam intensity of 10^8 lead ions in a 5 sec spill, a SPS cycle time of 19.2 sec, a 4cm lead production target (equivalent to 1 interaction length) and an overall beam time efficiency $\varepsilon = 0.5$, we expect to obtain $2 \cdot 10^{12}$ interactions in 14 days of running. The corresponding strangelet sensitivities $S \cdot Z$ versus m/Z for $<p_t> = 0.1\sqrt{m}$ GeV/c are shown in Fig.9 for three different spectrometer rigidities. The largest m/Z range would be covered by the R = 200GV spectrometer rigidity setting.

The principle experimental method for a strangelet search described above has been successfully tested in S-W collisions at 200 GeV/c per nucleon during a test run in April 1992 at CERN. As a result, sensitivities of 10^{-6} to 10^{-7} per interaction, have been obtained for negatively and positively charged strangelets over a large mass range [12].

9. Conclusions

An interesting new generation of strangelet search experiments are forthcoming in the near future at BNL with Au-beams and at CERN with Pb-beams. Together with the new balloon experiment of the Italian Japanese

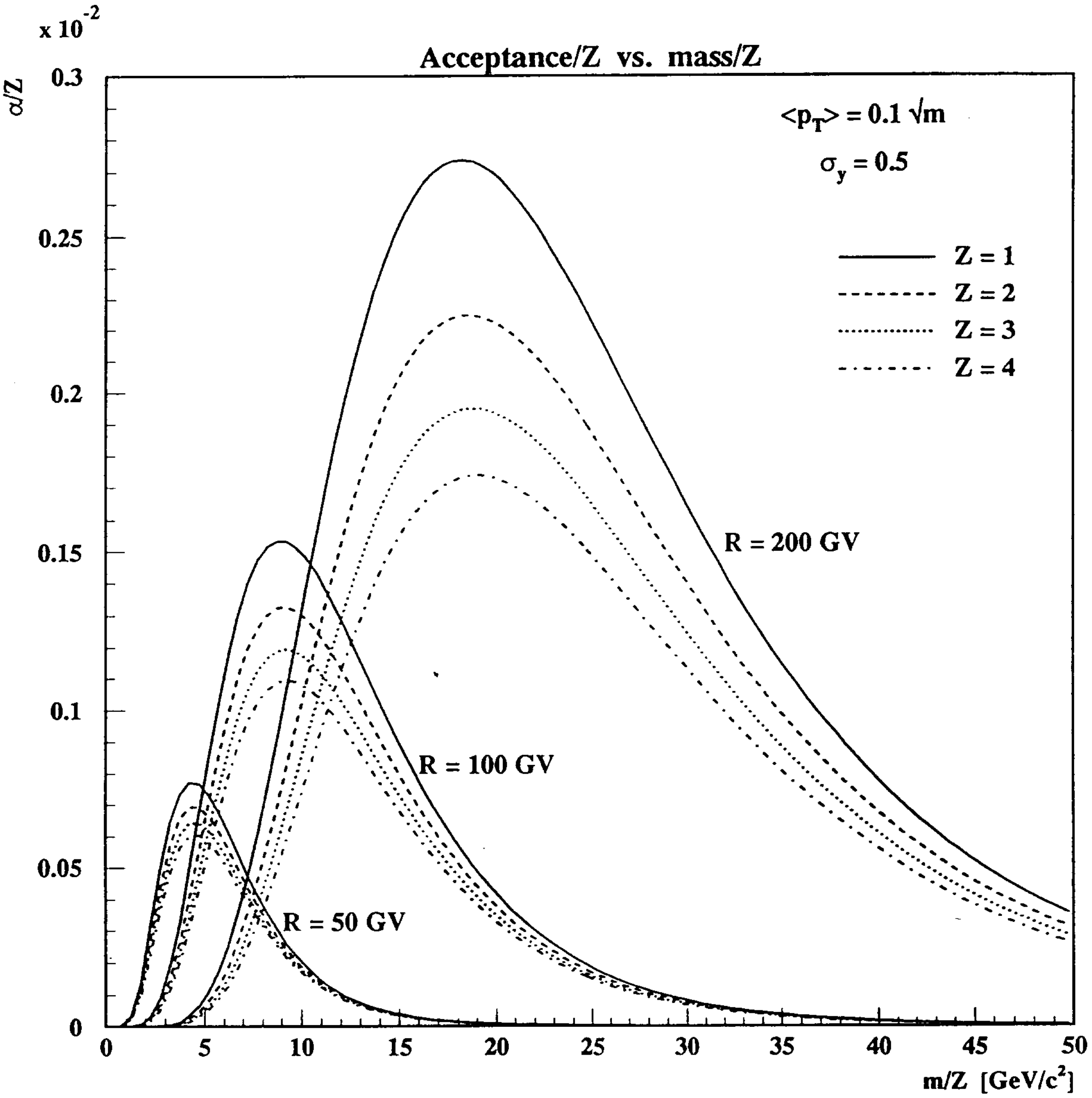

Fig.8 H6 beam spectrometer acceptance α / Z versus m/Z for 0° production angle and rigidities R=50, 100, 200GV.

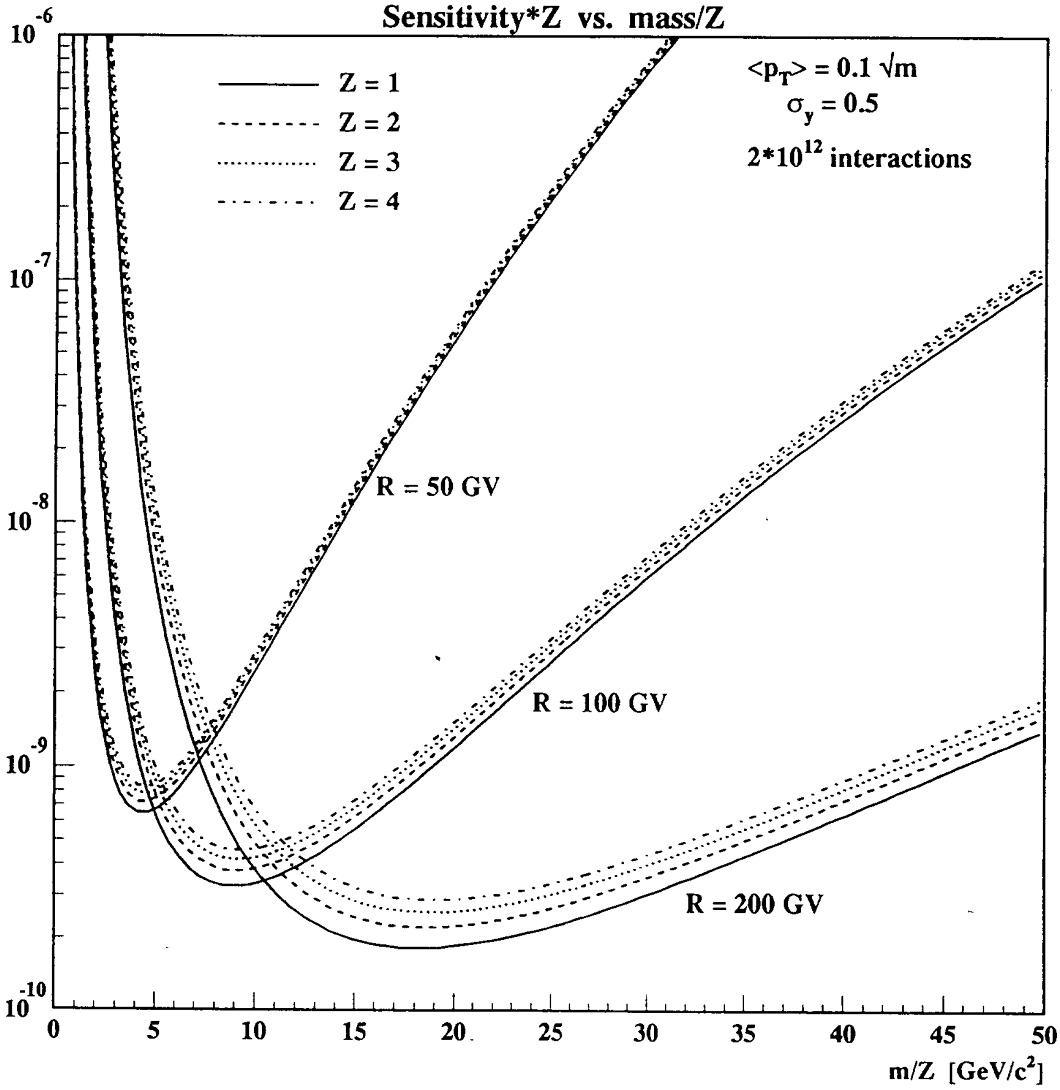

Fig.9 Detection sensitivity $S \cdot Z$ of strangelets at 0^0 production angle and $<p_t> = 0.1\sqrt{m}$ GeV/c for spectrometer rigidities R=50, 100, 200GV are shown as a function of m/Z.

Collaboration they hopefully will lead to the discovery of strange quark matter.

References

[1] H.C. Liu and G. Shaw *Phys.Rev.* **D30 N5** (1984) 1137.

[2] C. Greiner, P. Koch and H. Stoecker, *Phys.Rev.Lett.* **58 N18** (1987) 1825, see also contributions of H. Stoecker in these proceedings.

[3] E. Witten, *Phys.Rev.* **D30 N2** (1984) 272.

[4] See contributions of C. Alcock, H. Heiselberg, M. Rho and F. Weber in these proceedings.

[5] J.D. Bjorken and L.D. McLerran, *Phys.Rev.* **D20** (1979) 2353, see also contributions of E. Gladysz-Dziadus in these proceedings.

[6] B. S. Kumar in "The Physics and Astrophysics of Quark-Gluon Plasmas", Proceedings, edited by B. Sinha, Y.P. Viyogi and S. Raha *World Scientific* (1994) 63, see also contributions of B.S. Kumar and H. Crawford in these proceedings.

[7] T. Saito et al., *Phys.Rev.Lett.* **65** (1990) 2094, see also contributions of T. Saito in these proceedings.

[8] K. Borer et al., Proposal for a *Strangelet and Particle Search in Lead Lead Collisions* **CERN/SPSLC/P268** (1992), see also Q.P. Zhang in these proceedings.

[9] G. d'Agostini et al., *NIM* **A274** (1989) 134.

[10] H.J. Crawford, M.S. Desai and G.L. Shaw, *Phys.Rev.* **D45** (1992) 827.

[11] A. Bamberger et al., *Nuclear Phys.* **A498** (1989) 133c-150c.

[12] K. Borer et al., *Phys.Rev.Lett.* **72 N10** (1994) 1415.